Sensors and Actuators B 145 (2010) 702–707

Contents lists available at ScienceDirect

Sensors and Actuators B: Chemical

journal homepage: www.elsevier.com/locate/snb

Hg(II) sensing based on functionalized carbon dots obtained by direct laser ablation

Helena Gonçalves[a], Pedro A.S. Jorge[b], J.R.A. Fernandes[b,c], Joaquim C.G. Esteves da Silva[a,*]

[a] Centro de Investigação em Química, Departamento de Química, Faculdade de Ciências da Universidade do Porto, R. Campo Alegre 687, 4169-007 Porto, Portugal
[b] Optoelectronics Unit, INESC Porto, R. Campo Alegre 687, 4169-007 Porto, Portugal
[c] Universidade de Trás-os-Montes e Alto Douro, Apartado 1013, 5001-801 Vila Real, Portugal

ARTICLE INFO

Article history:
Received 9 December 2009
Received in revised form 13 January 2010
Accepted 15 January 2010
Available online 25 January 2010

Keywords:
Carbon nanoparticles
Carbon dots
Laser ablation
Functionalization
N-acetyl-L-cysteine
Mercury(II) sensing

ABSTRACT

The synthesis of carbon nanoparticles obtained by direct laser ablation [UV pulsed laser irradiation (248 nm, KrF)] of carbon targets immersed in water is described. Laser ablation features were optimized to produce carbon nanoparticles with dimensions up to about 100 nm. After functionalization with NH_2–polyethylene-glycol (PEG_{200}) and N-acetyl-L-cysteine (NAC) the carbon nanoparticles become fluorescent with excitation and emission wavelengths at 340 and 450 nm, respectively. The fluorescence decay time was complex and a three-component decay time model originated a good fit ($\chi = 1.09$) with the following lifetimes: $\tau_1 = 0.35$ ns; $\tau_2 = 1.8$ ns; and $\tau_3 = 4.39$ ns. The fluorescence of the carbon dots is sensitive to pH with an apparent $pK_a = 4.2$. The carbon dots were characterized by ^{1}H NMR and HSQC and the results show an interaction between PEG_{200} and the carbon surface as well as a dependence of the chemical shift with the reaction time. The fluorescence intensity of the nanoparticles is quenched by the presence of Hg(II) and Cu(II) ions with a Stern–Volmer constant (pH = 6.8) of 1.3×10^5 and 5.6×10^4 M^{-1}, respectively. As such the synthesis and application of a novel biocompatible nanosensor for measuring Hg(II) is presented.

1. Introduction

Quantum dots (QDs) are nanoparticles (typically between 1 and 12 nm in diameter) of semi-conducting material. Due to the quantum confinement effects, these materials possess unique light emitting properties, like a broad excitation spectra and a sharp emission wavelength that can be tuned by controlling the reaction time. In the last decade they have revealed to be a powerful tool for labeling biological systems since their nanoscale size range is compatible to most of the metabolic and internalization processes observed in cells [1–3] and, unlike other nanoparticle-based optical imaging probes, QDs do not exceed the protein's size [4], which makes them highly interesting for biological applications. Carbon dots, show some common properties to QDs, but are carbon nanoparticles that through functionalization acquire strong photoluminescence in both solution and solid state. In general, the photoluminescence has been attributed to the presence of surface energy traps, likely related to the abundant surface defect sites that become emissive upon functionalization. In addition, the surface emissive sites of the carbon dots are likely quantum confined in the sense that a large surface-to-volume ratio is required for the strong photoluminescence [5–8]. With emission properties similar to those described for the traditional cadmium based QDs, these carbon dots represent a possibility of performing *in vivo* measurements in a non-invasive and non-toxic manner. Moreover, carbon dots are able to emit visible light after two-photon excitation using near infrared light which makes them particularly interesting material for the development of *in vivo* imaging applications [9,10]. Since they can be functionalized with several molecules in a number of layers accordingly with the desirable application [11], these nanoparticles show great potential for *in vivo* fluorescence sensing applications.

Herein we report a straightforward synthesis of carbon dots by laser ablation (UV pulsed laser irradiation) of carbon targets immersed in water and their functionalization with NH_2–polyethylene-glycol (PEG_{200}) and N-acetyl-L-cysteine (NAC). It was recently shown that using QDs capped with PEG_{200} in cultured keratinocytes significantly inhibited cytotoxicity and immune responses when compared with QDs without this capping [12]. These results suggest that PEG coating is an effective approach for the safe use of QDs for *in vivo* applications [13,14]. On the other hand NAC is a metabolite of the sulfur-containing amino acid, cysteine and is produced within the human body. Metals like lead, mercury and arsenic are detoxified and removed from the body by NAC [15]; therefore we tested the sensitivity of the synthesized carbon dots towards metal ions.

* Corresponding author. Tel.: +351 220 402 569; fax: +351 220 402 659.
E-mail address: jcsilva@fc.up.pt (J.C.G. Esteves da Silva).

0925-4005/$ – see front matter © 2010 Elsevier B.V. All rights reserved.
doi:10.1016/j.snb.2010.01.031

2. Experimental

2.1. Synthesis and functionalization of CNP

All chemicals were purchased from Sigma–Aldrich and were used without further purification. The ablation process was implemented using UV pulsed laser irradiation (248 nm, KrF) of carbon targets immersed in water.

The functionalization process was adapted from [16] and it is constituted by three steps:

(i) *Activation of carbon nanoparticles* – 20 mL of the water solution with the nanoparticles dispersed plus 20 mL of HNO_3 (0.1 M) were refluxed for 12 h.
(ii) *Functionalization with PEG*$_{200}$ – solution from (i) plus 20 mL of PEG_{200} were refluxed for 28 h.
(iii) *Functionalization with N-acetyl-L-cysteine (NAC)* – solution from (ii) plus 2.984 g of NAC were refluxed for 31 h. The solution goes from colorless to yellow-brown.

The obtained carbon dots solution was extracted six times with ethyl acetate in order to eliminate unreacted reagents. 1 mL of this purified solution was diluted in a 100 mL flask which constituted the sensing solution used throughout the work. For the ^{1}H NMR and HSQC analyses the carbon dots were dried in vacuum for 1 h before dilution with deuterated water.

2.2. pH and metal ion titrations

The pH of the sensing solution was adjusted to 5.0 ± 0.1, 6.8 ± 0.1 and 8.0 ± 0.1 using phosphate buffer solutions and the addition of micromolar quantities of all metal ions did not change this value.

Standard aqueous solutions of $Hg(NO_3)_2$, $Pb(NO_3)_2$, $CdCl_2$, $Cu(NO_3)_2$, $NiCl_2$, $CoCl_2$ and $Zn(NO_3)_2{\cdot}4H_2O$ from Merck, were prepared in water with concentrations of 5.00×10^{-4} M. Aliquots of these standard solutions were added to 20 mL of carbon dots solution at pH 6.8 – 25 mL of the solution A and 25 mL of phosphate buffer solution at pH 6.8 – in order to obtain the following metal ions concentrations: 1.00×10^{-7}, 5.99×10^{-7}, 1.30×10^{-6}, 1.99×10^{-6}, 1.30×10^{-6}, 2.69×10^{-6} M. Hg(II) was subjected to a detailed analysis and a series of solutions in the range up to 3.60×10^{-6} M were prepared.

2.3. Instrumentation

Excitation emission matrices of fluorescence (EEM) [excitation between 199.4 and 672.8 nm and emission between 349.7 and 719.7 nm] were obtained with a Spex 3D luminescence spectrophotometer equipped with a Xenon pulse discharge lamp (75 W) and a CCD detector, 0.25 mm slits and 1 s integration time were used. Lifetime measurements were recorded with a Horiba Jovin Yvon Fluoromax 4 TCSPC using the following instrumental settings: 368 nm NanoLED; time range, 200 ns; peak preset 10,000 counts; repetition rate at 1 MHz; synchronous delay of 50 ns; emission detection of 550 nm. Quartz cuvettes were used.

Scanning electron microscopy (SEM) and X-ray analysis of the three purified carbon dots were done on a FEI Quanta 400FEG/EDAX Genesis X4M High Resolution Scanning Electronic Microscope.

NMR characterization was performed in D_2O for both ^{1}H NMR (500.13 MHz) and HSQC, on a Bruker-AMX500 spectrometer at 298 K. PEG_{200}, NAC and the synthesized carbon dots were characterized by ^{1}H NMR spectrometry (500 MHz, D_2O): PEG_{200}: δ = 3.66–3.68 (m, 36H), 3.740–3.742 (m, 110H); NAC: δ = 1.99 (s, 3H), 2.89–2.91 (m, 2H), 4.53–4.56 (t, 1H); carbon nanoparticles + PEG_{200}: δ = 2.91–3.02 (m, 92H), 3.51 (m, 2H), 4.61 (s, 1H); carbon nanoparticles + PEG_{200} + NAC 1 h: δ = 1.82–1.88 (m, 7H), 3.38–3.55 (m, 264H), 3.95–4.11 (m, 11H); carbon nanoparticles + PEG_{200} + NAC 31 h: δ = 1.82–1.88 (m, 15H), 2.73 (s, 5H), 3.38–3.55 (m, 376H), 3.95–4.10 (m, 15H), 4.37–4.40 (m, 4H), 8.00 (s, 1H).

The size distribution of carbon dots in water was determined by dynamic light scattering analysis using a Malvern Instruments (Malvern, UK) Zeta Sizer Nano ZS, using disposable polystyrene cells from Sigma.

2.4. Data analysis

Lifetime deconvolution analysis was done using Decay Analysis Software v6.4.1 (Horiba Jovin Yvon). Fluorescence decays were interpreted in terms of a multiexponential model:

$$I(t) = A + \sum B_i \exp\left(-\frac{t}{\tau_i}\right)$$

where B_i are the pre-exponential factors and τ_i the decay times. The fraction contribution (percentage of photons) of each decay time component is represented by B_i.

Although carbon dots show a polyelectrolyte behavior the variation of its fluorescence intensity resulting from the ionization reaction can be linearized using a Henderson–Hasselbach type equation which allows the calculation of an apparent pK_a.

$$\mathrm{pH} = \mathrm{p}K_a + n \log\left[\frac{I_{max} - I}{I - I_{min}}\right]$$

where I_{max} and I_{min} are respectively the maximum and minimum of the fluorescence intensity of the acid or conjugated base species and I is the fluorescence intensity as function of the pH. For a polyelectrolyte the slope of the plot of pH as function of $\log[(I_{max} - I)/(I - I_{min})]$, n, is an empirical parameter usually greater than unity [17].

In this study static quenching of fluorescence by metal ions [M(II)] was described using the Stern–Volmer equation:

$$\frac{I_o}{I} = 1 + K_{SV}[\mathrm{M(II)}]$$

where I_o is the fluorescence intensity without metal ion, I is the fluorescence intensity observed in the presence of a metal ion and K_{SV} is the static (conditional stability constant) Stern–Volmer constant [18].

3. Results and discussion

3.1. Synthesis and morphological characterization

The synthesis of the carbon nanoparticles was performed in deionized water using a similar but simplified strategy to one previously described [16]. The carbon targets were irradiated for 1 min and no support method to expedite the movement of the generated nanoparticles was used. Literature described synthesis of carbon nanoparticles used ultrasounds and the carbon targets were irradiated for several hours using a system apparatus far more complex than the one used in this work [16,19].

A pulsed UV laser (Lambda Physik LPX 300i – 248 nm KrF) was used to irradiate the carbon targets and a positive lens of +50 cm of focal distance was used to change the area illuminated by the laser. In all experiments the same energy (400 mJ) and repetition rate (10 Hz) were used. It was also maintained the same distance between the carbon target and the water surface and all experiments occurred at room temperature.

To optimize the laser ablation procedure, the area of the irradiated carbon target was changed and the size dispersion of the resulting nanoparticles was evaluated by SEM. When the distance between the focusing lens and the carbon target was 107 cm, the incidence area of the laser was of 348 mm^2 resulting in a fluence of

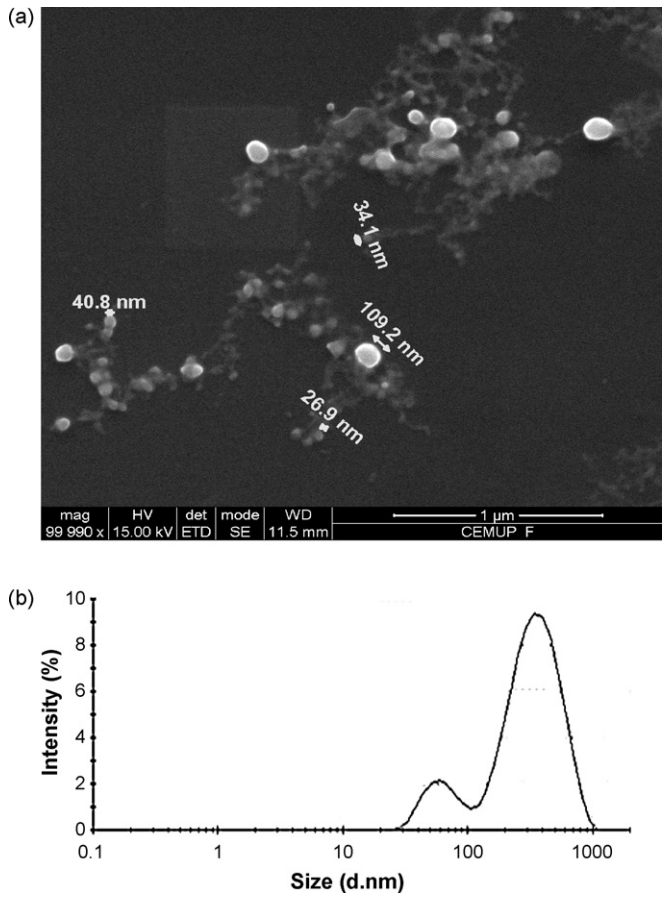

Fig. 1. (a) SEM image in a TEM grid and (b) DLS size dispersion of the carbon particles produced by laser ablation.

115 mJ/cm^2. In these conditions, the carbon particles obtained have wide size dispersion – however, the most predominant are in the hundred nanometers range. On the other hand, when the distance between the focusing lens and the carbon target was set to 85 cm, the laser area of incidence was 139 mm^2 resulting in a fluence of 288 mJ/cm^2, smaller particles were produced with dimensions down to about 27 nm (Fig. 1a). Fig. 1b shows the DLS of the nanoparticles obtained by direct laser ablation which shows two major average size dispersions centred at values of 63 and 373 nm – the smaller particles were probably obtained from laser ablation of the bigger particles. Since the objective is to synthesize nanosensors these conditions were used for further studies.

The carbon nanoparticles obtained by laser ablation are not fluorescent. In order to make them fluorescent it was necessary first to activate the carbon surface by refluxing the carbon nanoparticles in nitric acid for 12 h and, afterwards, add PEG_{200}. After 1 h reaction with PEG_{200} the carbon dots exhibited a pale yellow color and fluorescence with an emission wavelength of 565 nm. After 28 h reaction, NAC was added to the reaction mixture and samples of the reaction medium were taken over time in order to control the wavelength and intensity variation. The samples taken during the functionalization reaction showed an emission wavelength variation of 20 nm towards the red and an increase in fluorescence. The reaction ended after 31 h when the fluorescence intensity started to decrease which corresponded to the maximum nanoparticle size and quantum confinement.

The resulting solution contains carbon dots functionalized with PEG_{200} and NAC and could not be dried, limiting the possibility of electron microscopy analysis. Alternatively, carbon dots were characterized by NMR.

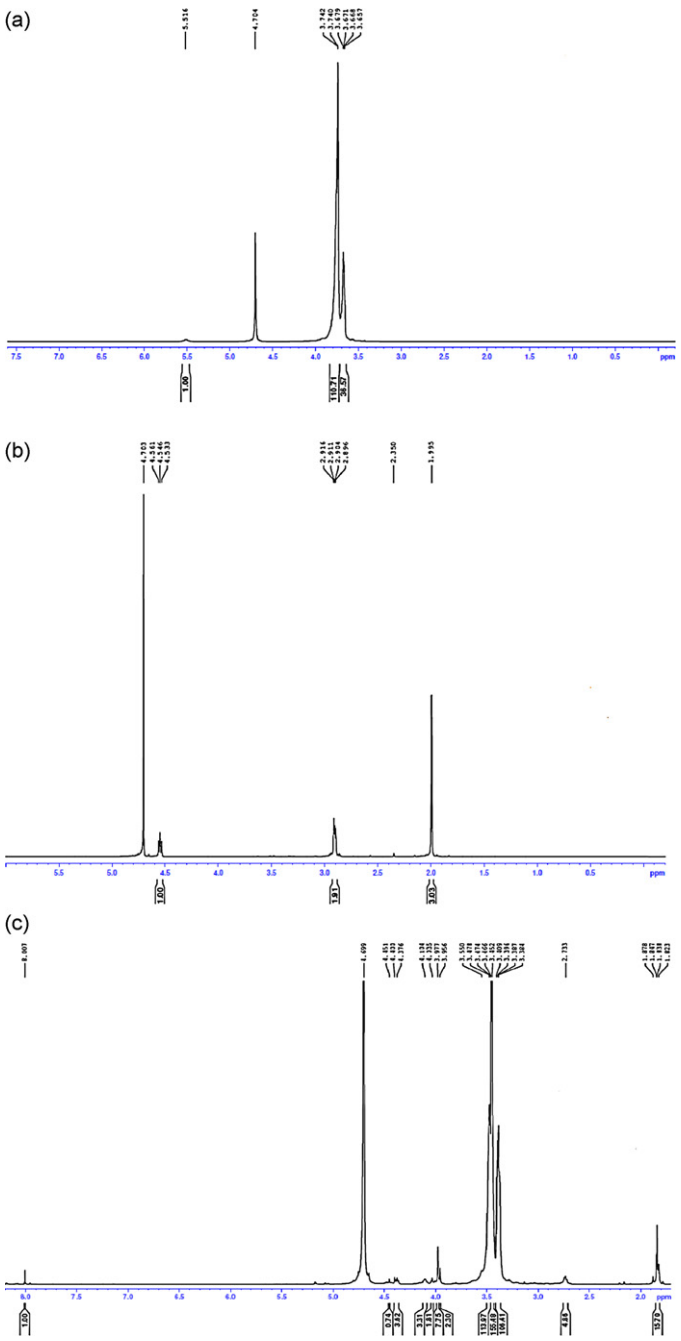

Fig. 2. ^{1}H NMR spectra of (a) PEG_{200}, (b) NAC and (c) carbon nanoparticles + PEG_{200} + NAC 31 h reaction time in D_2O.

3.2. NMR analysis

NMR analysis of the carbon dots were performed in D_2O. In order to follow the reaction samples of PEG_{200}, NAC and samples of carbon nanoparticles + PEG_{200} 1 h reaction, carbon nanoparticles + PEG_{200} + NAC 1 h reaction, and carbon nanoparticles + PEG_{200} + NAC 31 h reaction were analyzed by ^{1}H NMR (Fig. 2 and Supplementary material) and HSQC (Supplementary material). The analysis of the evolution of the chemical shifts, and respective multiplicity, due to PEG_{200} and NAC during the reaction time in the presence of the carbon nanoparticles suggests the formation of covalent bonds among all the species.

The analysis of the NMR spectra of carbon nanoparticles with PEG_{200} sample after 1 h reaction shows a chemical shift to lower

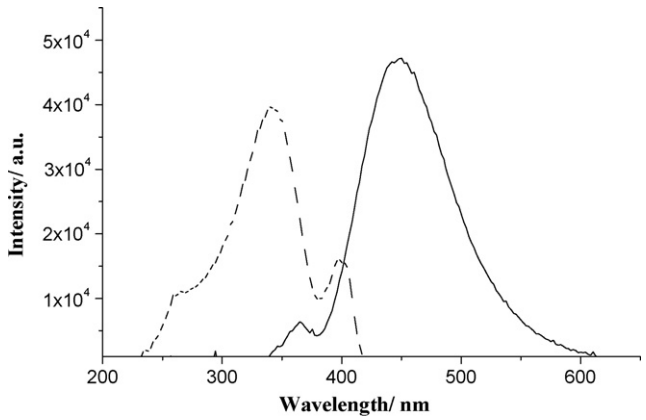

Fig. 3. Fluorescence excitation (– – –) and emission (—) spectra of the carbon dots.

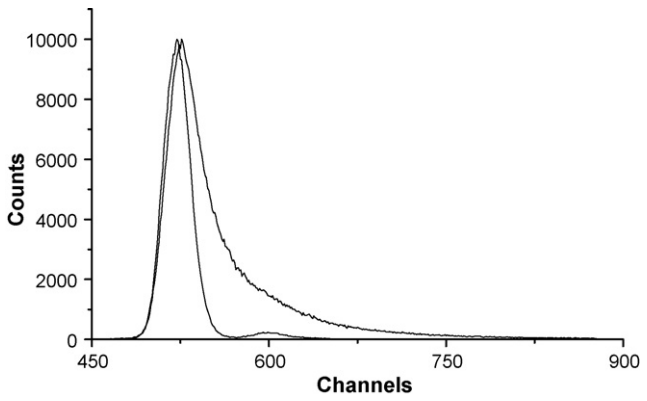

Fig. 4. Fluorescence decay of aqueous carbon dots.

values of all the signals attributed to PEG protons. This evolution of the chemical shift indicates a stabilization of the molecule, probably due to the interaction between the carbon dots surface and the PEG residue. Also the multiplet that in pure PEG (Fig. 2) appeared well defined at 3.7 ppm is now being split into two probably due to the proximity effect of several PEG molecules on the carbon dots surface.

Upon addition of NAC and after 1 h reaction the signal from the PEG and NAC protons shifted to higher values. This evolution of the chemical shift indicates an interaction between the PEG and NAC residues. This hypothesis is supported by the analysis of the signal at 1.8 ppm from the R-$COCH_3$ that typically is a singlet but, due to the presence of other non-equivalent protons, becomes a multiplet (Fig. 2). After 31 h reaction it is still possible to see PEG protons that remained at 3.9 ppm, indicating that the PEG_{200} was in excess but also that the residues that are interacting with the dots surface are probably more stable, therefore appearing at lower chemical shifts. The analysis of the HSQC data (Supplementary material) supported the observations of ^{1}H NMR.

3.3. Fluorescent properties of the carbon dots

The excitation and emission spectra of the synthesized carbon dots functionalized with PEG_{200} and NAC are shown in Fig. 3. The maximum excitation and emission are located at 340 and 450 nm, respectively, with a Stokes shift of about 110 nm.

This Stokes shift is superior than the one previously reported [13] of 70 nm (excitation maximum at 420 nm and emission at 490 nm) for the carbon dots functionalized only with PEG_{200} indicating not only that the reaction time is important to obtain higher emission and Stokes shifts values; but also that the presence of two different molecules (NAC and PEG_{200}) on the nanoparticles surface affects the quantum yield and quantum confinement. These variations on the emission wavelength with the reaction time suggest that the carbon dots are increasing their size and that the two functionalization molecules interact with their surface affecting the quantum confinement [20,21].

A typical fluorescence decay time profile of the carbon dots is shown in Fig. 4. The preliminary analysis of the decay time indicates that it is complex as it shows the presence of several lifetime ranges. Indeed, only a three-component decay time model originated a good fit ($\chi = 1.09$) with the following lifetimes: $\tau_1 = 0.35$ ns; $\tau_2 = 1.8$ ns; and $\tau_3 = 4.39$ ns (Table 1).

Table 1
Lifetime intensity decays of carbon dots in water[a].

N	τ_i (ns)	α_i	f_i	
1	0.35(0.02)	0.0958(0.0006)	30.6%	
2	1.8(0.1)	0.0263(0.0002)	42.2%	
3	4.39(0.05)	0.00673(0.00005)	27.1%	$\chi = 1.09$

[a] Standard deviation in parenthesis.

3.4. Effect of the pH and metal ions on the fluorescence of CNP

After functionalization with PEG_{200} and NAC it was observed that the fluorescence of the carbon dots was sensitive to pH (Fig. 5). This sensitivity is marked by a decrease of the fluorescence intensity as the pH increases and, by fitting the fluorescence intensities with the Henderson–Hasselbach equation, it was found an apparent pK_a of 4.2 ± 0.1 and a slope of 2.5. This pH behavior is reversible. Also, as the slope is higher than unity it suggests that the carbon dots follow a polyelectrolyte ionization.

This variation is due to the ionization of the acid groups of the NAC residue of the carbon dots which may influence the confinement energy of the nanoparticles resulting in a variation of the fluorescence. Since the carbon dots presented sensitivity towards the pH, when we passed on to the quenching assays it was necessary to perform a preliminary study in order to determine the appropriate pH to do such studies. For these assays it was studied the quenching effect of Hg(II) on the synthesized carbon dots at pH 5.0, 6.8 and 8.0. At pH 5.0 a white precipitate was found which eliminated this pH for further studies. At pH 8.0 the intensity signal was better than at pH 6.8, however the quenching effect on the carbon dots was negligible, when compared to the signal observed at pH 6.8. Accordingly to these results the quenching effect of the metal ions was performed in a buffered phosphate solution at pH 6.8. This pH quenching dependence is due to the hydrolysis of the mercury

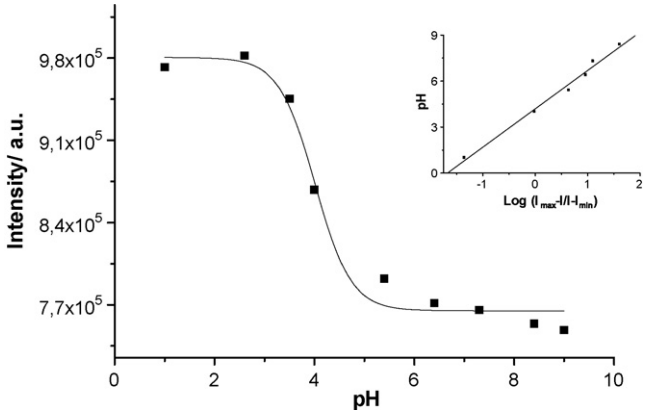

Fig. 5. Variation of the fluorescence intensity of aqueous carbon dots as a function of the pH.

Table 2
Stern–Volmer parameters for the quenching of carbon dots by Hg(II) and Cu(II) ions[a].

Ion	K_{SV} (M^{-1})	Intercept	R	Points	Concentration range (M)
Hg(II)	$1.3(0.4) \times 10^5$	0.97(0.01)	0.9719	17	1.00×10^{-7}–2.69×10^{-6}
Cu(II)	$5.6(0.8) \times 10^4$	1.0(0.2)	0.9607	6	1.00×10^{-7}–2.69×10^{-6}

[a] Averages and standard deviation (in parenthesis) of three independent experiences. R, correlation coefficient.

ions [22]. Indeed, although the total mercury concentration is quite low, at pH 8.0 the $Hg(OH)_2$ species is quantitatively formed and the NAC is not able to complex the mercury. At pH 6.8, the $[Hg(OH)]^+$ species is probably the main mercury species in aqueous solution and it is available to be complexed by the carbon dots.

Since the carbon dots were functionalized with NAC, it is expected that their fluorescence properties would change when they react with metal ions. Several metal ions [Hg(II), Cu(II), Cd(II), Ni(II), Zn(II) and Ca(II)] were tested to check if they affect the fluorescence properties of the carbon dots.

As shown in Fig. 6 the carbon dots fluorescence is affected by Hg(II), where it is possible to observe a marked quenching effect – the fluorescence signal decreases 25% upon addition of micromolar concentration of Hg(II) (2.69×10^{-6} M). The addition of Cu(II) also provokes quenching of the fluorescence of the carbon dots but in less extent than with Hg(II) – about 13% decrease is observed. The other metal ions analyzed, namely Cd(II), Ni(II), Zn(II) and Ca(II), show no measurable effect on the fluorescence of the carbon dots.

The quenching provoked by Hg(II) is described as a typical Stern–Volmer plot (Fig. 7). Table 2 presents the parameters of the linear fitting of the quenching provoked by Hg(II) and Cu(II). The analysis of the Stern–Volmer plots show that they follow a linear trend with $K_{SV} = 1.3(4) \times 10^5$ and $5.6(8) \times 10^4$ for Hg(II) and Cu(II), respectively. This order of magnitude is compatible with the formation of a quite stable complexes (static quenching) between the NAC residues on the surface of the carbon dots and Hg(II) and Cu(II) ions.

In order to access if the quenching effect is due to the NAC or the PEG residue, a study was performed using the nanoparticles functionalized only with PEG (Supplementary material) and it was found that there is no significant fluorescence emission or intensity variations upon addition of the same micromolar concentration of Hg(II). As such, and as expected, the sensitivity towards Hg(II) (soft donor) is due to the NAC residue (namely the sulfur atom – soft acceptor) of the carbon dots.

A variety of analytical tools are commonly employed to detect mercury in biological samples [23–27]. However while traditional

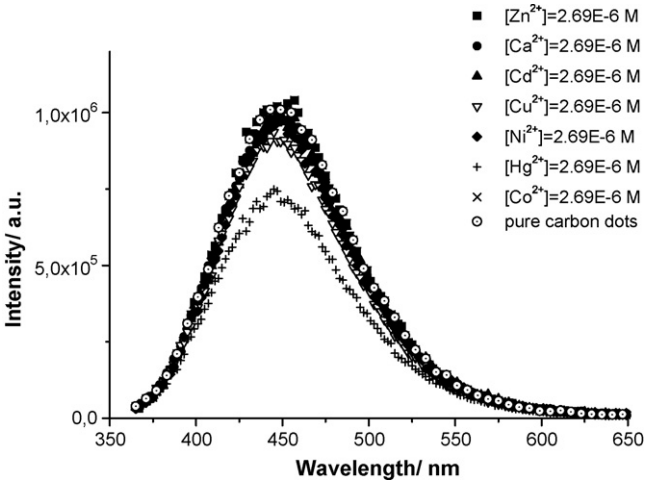

Fig. 6. Fluorescence quenching of the synthesized carbon dots in aqueous solution by 2.69×10^{-6} M of all metal ions.

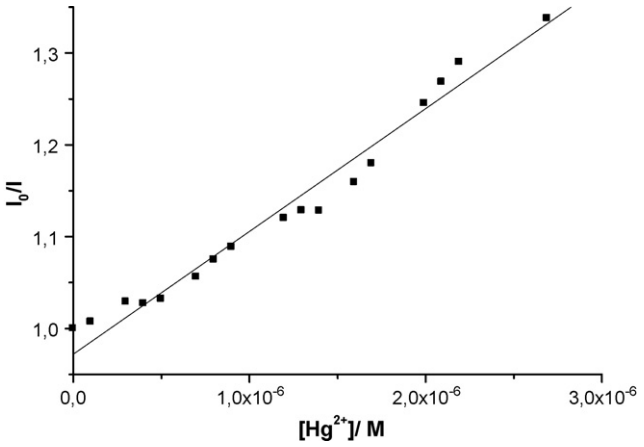

Fig. 7. Stern–Volmer plot of the fluorescence quenching of carbon dots in aqueous solution by Hg(II).

analytical detection methods allow detection limits in the nanomolar range [28–30], they commonly do not allow time-dependent or location-specific *in vivo* measurements. As the uptake and distribution of this heavy metal are not understood, highly sensitive and non-invasive methods are needed for its detection in a living organism.

Herein these carbon dots are of great importance due not only to their nanometer size and fluorescence properties but also because they can be specifically targeted in order to perform *in vivo* measurements in a non-invasive way, thereby representing a novel non-toxic nanoanalytical tool.

4. Conclusions

The use of direct laser ablation to produce carbon nanoparticles in water rendered a wide variety of sizes accordingly with the laser fluence. As such, by controlling the energy and incidence area it is possible to produce particles in tens of nanometer range. These nanoparticles can easily be functionalized using more than one molecule and remain stable in an aqueous solution. Due to this stability it is also possible to immobilize them in the optical fiber devices using the sol–gel technique, which would render a specific optical nanoanalytical sensor. The functionalization using PEG_{200} and NAC allowed us to synthesize a nanosensor sensitive to micromolar concentrations of Hg(II) and Cu(II) as well as the solution pH. Since these carbon dots are biologically inert they are a promising solution for *in vivo* measurements of the mercury uptake dynamics. However, for the *in vivo* analysis of metal ions further research is needed to study the effect of biological molecules on the speciation of the metal ions (cysteine residuals, water soluble proteins, other anionic cellular components, etc.) in the presence of the carbon dots.

Acknowledgements

Financial support from Fundação para a Ciência e Tecnologia (Lisboa) (FSE-FEDER) (Project PTDC/QUI/71001/2006) is acknowledged. A PhD grant to Helena Gonçalves SFRH/BD/46406/2008 is acknowledged to Fundação para a Ciência e Tecnologia (Lisboa).

Appendix A. Supplementary data

Supplementary data associated with this article can be found, in the online version, at doi:10.1016/j.snb.2010.01.031.

References

[1] D. Gerion, F. Pinaud, S.C. Williams, W.J. Parak, D. Zanchet, S. Weiss, A.P. Alivisatos, Synthesis and properties of biocompatible water-soluble silica-coated CdSe/ZnS semiconductor quantum dots, J. Phys. Chem. B 105 (2001) 8861–8871.

[2] A.N. Rogach, D. Nagesha, J.W. Ostrander, M. Giersig, N.A. Kotov, "Raisin Bun"-type composite spheres of silica and semiconductor nanocrystals, Chem. Mater. 12 (2000) 2676–2685.

[3] Y. Williams, A. Sukhanova, M. Nowostawska, A.M. Davies, S. Mitchell, V. Oleinikov, Y. Gun'ko, I. Nabiev, D. Kelleher, Y. Volkov, Probing cell-type-specific intracellular nanoscale barriers using size-tuned quantum dots, Small 5 (2009) 2581–2588.

[4] M.J. Murcia, D.L. Shaw, E.C. Long, C.A. Naumann, Fluorescence correlation spectroscopy of CdSe/ZnS quantum dot optical bioimaging probes with ultra-thin biocompatible coatings, Opt. Commun. 281 (2008) 1771–1780.

[5] P. Juzenas, W. Chen, Y.-P. Sun, M.A.N. Coelho, R. Generalov, N. Generalova, I.L. Christensen, Quantum dots and nanoparticles for photodynamic and radiation therapies of cancer, Adv. Drug Deliv. Rev. 60 (2008) 1600–1614.

[6] J. Lia, D. Baoa, X. Honga, D. Li, J. Li, Y. Baia, T. Lia, Luminescent CdTe quantum dots and nanorods as metal ion probes, Colloids Surf. A: Physicochem. Eng. Aspects 257–258 (2005) 267–271.

[7] C. Sun, B. Liu, J. Li, Sensitized chemiluminescence of CdTe quantum-dots on Ce(IV)-sulfite and its analytical applications, Talanta 75 (2008) 447–454.

[8] Z. Wang, J. Li, B. Liu, J. Li, CdTe nanocrystals sensitized chemiluminescence and the analytical application, Talanta 77 (2009) 1050–1056.

[9] P.T.C. So, Two-photon fluorescence light microscopy, in: Encyclopedia of Life Sciences, Macmillan Publishers Ltd, Nature Publishing Group, 2002, www.els.net.

[10] S.-T. Yang, X. Wang, H. Wang, F. Lu, P.G. Luo, L. Cao, M.J. Meziani, J.-H. Liu, Y. Liu, M. Chen, Y. Huang, Y.-P. Sun, J. Phys. Chem. C (2009), doi:10.1021/jp9085969.

[11] A.M. Smith, H. Duan, A.M. Mohs, S. Nie, Bioconjugated quantum dots for in vivo molecular and cellular imaging, Adv. Drug Deliv. Rev. 60 (2008) 1226–1240.

[12] J.P. Ryman-Rasmussen, Surface coatings determine cytotoxicity and irritation potential of quantum dot nanoparticles in epidermal keratinocytes, J. Invest. Dermatol. 127 (2007) 143–153.

[13] Y. Higuchi, Mannosylated semiconductor quantum dots for the labeling of macrophages, J. Control. Rel. 125 (2008) 131–136.

[14] A.C. Faure, S. Dufort, V. Josserand, P. Perriat, J.L. Coll, S. Roux, O. Tillement, Control of the in vivo biodistribution of hybrid nanoparticles with different poly(ethylene glycol) coatings, Small 5 (2009) 2565–2575.

[15] E. Raspanti, S.O. Cacciola, C. Gotor, L.C. Romero, I. García, Implications of cysteine metabolism in the heavy metal response in *Trichoderma harzianum* and in three *Fusarium* species, Chemosphere 76 (2009) 48–54.

[16] S.-L. Hu, K.-Y. Niu, J. Sun, J. Yang, N.-Q. Zhao, X.-W. Du, One-step synthesis of fluorescent carbon nanoparticles by laser irradiation, J. Mater. Chem. 19 (2009) 484–488.

[17] Q.Z. Wang, X.G. Chen, N. Liu, S.X. Wang, C.S. Liu, X.H. Meng, C.G. Liu, Protonation constants of chitosan with different molecular weight and degree of deacetylation, Carbohydrate Polym. 65 (2006) 194–201.

[18] J.R. Lakowicz, Principles of Fluorescence Spectroscopy, Kluwer-Plenum, New York, 1999 (Chapter 8).

[19] Y.-P. Sun, B. Zhou, Y. Lin, W. Wang, K.A.S. Fernando, P. Pathak, M.J. Meziani, B.A. Harruf, X. Wang, H. Wang, P.G. Luo, H. Yang, M.E. Kose, B. Chen, M. Veca, S.-Y. Xie, Quantum-sized carbon dots for bright and colorful photoluminescence, J. Am. Chem. Soc. 128 (2006) 7756–7757.

[20] C. Maule, H. Gonçalves, C. Mendonça, P. Sampaio, J.C.G. Esteves da Silva, P. Jorge, Wavelength encoded analytical imaging and fiber optic sensing with pH sensitive CdTe quantum dots, Talanta (2009), doi:10.1016/j.talanta.2009.10.048.

[21] J.M.M. Leitão, H. Gonçalves, C. Mendonça, J.C.G. Esteves da Silva, Multiway chemometric decomposition of EEM of fluorescence of CdTe quantum dots obtained as function of pH, Anal. Chim. Acta 628 (2008) 143–154.

[22] M.F. McComish, J.H. Ong, Trace metals, in: I. Bodek, W.J. Luman, W.F. Reehl, D.H. Rosenblatt (Eds.), Environmental Inorganic Chemistry, Pergamon Press, New York, 1988 (Chapter 7).

[23] R.R. Chapleau, R. Blomberg, P.C. Ford, M. Sagermann, Design of a highly specific and noninvasive biosensor suitable for real-time in vivo imaging of mercury (II) uptake, Protein Sci. 17 (2008) 614–622.

[24] L. Geiselhart, M. Osgood, D.S. Holmes, Construction and evaluation of a self-luminescent biosensor, Ann. N.Y. Acad. Sci. 646 (1991) 53–60.

[25] O. Selifonova, R. Burlage, T. Barkay, Bioluminescent sensors for detection of bioavailable Hg(II) in the environment, Appl. Environ. Microbiol. 59 (1993) 3083–3090.

[26] H. Yu, D. Mukhopadhyay, T.K. Misra, Purification and characterization of a novel organometallic receptor protein regulating the expression of the broad spectrum mercury-resistant operon of plasmid pDU1358, J. Biol. Chem. 269 (1994) 15697–15702.

[27] O.K. Lyngberg, D.J. Stemke, J.L. Schottel, M.C. Flickinger, A single-use luciferase-based mercury biosensor using *Escherichia coli* HB101 immobilized in a latex copolymer film, J. Ind. Microbiol. Biotechnol. 23 (1999) 668–676.

[28] H.N. Lee, H.N. Kim, K.M.K. Swamy, M.S. Park, J. Kim, H. Lee, K.-H. Lee, S. Park, J. Yoon, New acridine derivatives bearing immobilized azacrown or azathiocrown ligand as fluorescent chemosensors for Hg^{2+} and Cd^{2+}, Tetrahedron Lett. 49 (2008) 1261–1265.

[29] L. Guo, H. Hu, R. Sun, G. Chen, Highly sensitive fluorescent sensor for mercury ion based on photoinduced charge transfer between fluorophore and π-stacked T-Hg(II)–T base pairs, Talanta 79 (2009) 775–779.

[30] S Yoon, A.E. Alberts, A.P. Wong, C.J. Chang, Screening mercury levels in fish with a selective fluorescent chemosensor, J. Am. Chem. Soc. 127 (2005) 16030–16031.

Biographies

Helena Gonçalves obtained his B.Sc. and M.Sc. in chemistry from the Faculty of Sciences of the University of Porto (FCUP), Portugal, where she worked on the development of new bioanalytical sensors based new ruthenium and osmium complexes and CdTe quantum dots. Currently, she has a Ph.D. grant to work on the development of new bioconjugated and functionalized quantum and carbon dots.

Pedro A.S. Jorge graduated in applied physics (optics and lasers) from the University of Minho in 1996. He received his M.Sc. in optoelectronics and lasers from the physics department of the University of Porto in 2000. In 2006, he concluded his Ph.D. program at Porto University in collaboration with the department of physics and optical sciences at the University of Charlotte, North Carolina, USA, with work developed in luminescence based optical fiber. He is currently a senior researcher at INESC Porto, where he leads a small team in the development of biochemical sensors for environmental and medical applications.

J.R.A. Fernandes is a professor in the physics department of Universidade de Trás-os-Montes e Alto Douro and senior researcher at Optoelectronics Group of INESC Porto. He received his Ph.D. from Porto University. His research interests are in laser ablation of inorganic materials area for the production of thin films or for the production of nanoparticles to be used in sensors.

Joaquim C.G. Esteves da Silva obtained his B.Sc., M.Sc. and Ph.D. in chemistry from the Faculty of Sciences of the University of Porto (FCUP), Portugal, where he worked on chemometric methodologies to environmental inorganic systems. Currently, he is an associate professor in the chemistry and biochemistry department of the FCUP where he teaches inorganic, environment, forensic, bioanalytical and chemometric courses. His current main research interests are the development of fluorescent nanomaterials and enzymatic bioanalytical methods for biochemical, environmental and technological applications.